Dissipationless Anomalous Hall Current in the Ferromagnetic Spinel $CuCr_2Se_{4-x}Br_x$

Wei-Li Lee,[1] Satoshi Watauchi,[2]* V. L. Miller,[2] R. J. Cava,[2,3] N. P. Ong[1,3]†

In a ferromagnet, an applied electric field E invariably produces an anomalous Hall current J_H that flows perpendicular to the plane defined by E and M (the magnetization). For decades, the question of whether J_H is dissipationless (independent of the scattering rate) has been debated without experimental resolution. In the ferromagnetic spinel $CuCr_2Se_{4-x}Br_x$, the resistivity ρ (at low temperature) may be increased by several decades by varying *x* (Br) without degrading M. We show that J_H/E (normalized per carrier, at 5 kelvin) remains unchanged throughout. In addition to confirming the dissipationless nature of J_H, our finding has implications for the generation and study of spin-Hall currents in bulk samples.

A major unsettled question in the study of electron transport in a ferromagnet is whether the anomalous Hall current is dissipationless. In nonmagnetic metals, the familiar Hall current arises when electrons moving in crossed electric (**E**) and magnetic (**H**) fields are deflected by the Lorentz force. However, in a ferromagnet subject to **E** alone, a large, spontaneous (anomalous) Hall current $\mathbf{J}_H$ appears transverse to **E** (in practice, a weak **H** serves to align the magnetic domains) (*1*, *2*). Questions regarding the origin of $\mathbf{J}_H$, and whether it is dissipationless, have been keenly debated for decades. They have emerged anew because of fresh theoretical insights and strong interest in spin currents for spin-based electronics. We report measurements in the ferromagnet $CuCr_2Se_{4-x}Br_x$. Despite a 70-fold increase in the scattering rate from impurities, we found that $\mathbf{J}_H$ (per carrier) remains constant, implying that it is indeed dissipationless.

Karplus and Luttinger (*3*, *4*) proposed a purely quantum-mechanical origin for $\mathbf{J}_H$. An electron in the conduction band of a crystal lattice spends part of its time in nearby bands because of admixing caused by the (intracell) position operator **X**. In the process, it acquires a spin-dependent "anomalous velocity" (*5*). Karplus and Luttinger predicted that the Hall current is dissipationless: $\mathbf{J}_H$ remains constant even as the longitudinal current ($\mathbf{J}\|\mathbf{E}$) is degraded by scattering from added impurities. A conventional mechanism was later proposed (*6*) whereby the anomalous Hall effect (AHE) is caused instead by asymmetric scattering of electrons by impurities (skew scattering). Several authors (*7*–*9*) investigated the theoretical ramifications of these competing models. The role of impurities in the anomalous-velocity theory was clarified by Berger's side-jump model (*7*). A careful accounting of various contributions (including side-jump) to the AHE in a semiconductor has been given by Noziéres and Lewiner, who derived $\mathbf{X} = \lambda\mathbf{k} \times \mathbf{S}$, where λ is the enhanced spin-orbit parameter, **k** is the carrier wave vector, and **S** is its spin (*9*). In the zero-frequency limit, Noziéres and Lewiner obtained the AHE current

$$\mathbf{J}_H = 2ne^2\lambda\mathbf{E} \times \mathbf{S} \qquad (1)$$

where n is the carrier density and e is the charge. As noted, $\mathbf{J}_H$ is linear in **S** but is independent of the electron lifetime τ.

In modern terms, the anomalous-velocity term of Karplus and Luttinger is related to the Berry phase (*10*) and has been applied (*11*) to explain the AHE in Mn-doped GaAs (*12*). The close connection of the AHE to the Berry phase has also been explored in novel ferromagnets in which frustration leads to spin chirality (*13*–*15*). In the field of spintronics, several schemes have been proposed to produce a fully polarized spin current in thin-film structures (*16*) and in bulk *p*-doped GaAs (*17*). The AHE is intimately related to these schemes, and our experimental results are relevant to the spin current problem.

In an AHE experiment (*1*), the observed Hall resistivity ρ_{xy} comprises two terms,

$$\rho_{xy} = R_0B + \rho'_{xy} \qquad (2)$$

where B is the induction field, R_0 is the ordinary Hall coefficient, and ρ'_{xy} is the anomalous Hall resistivity. A direct test of the dissipationless nature of $\mathbf{J}_H$ is to check whether the anomalous Hall conductivity σ'_{xy} (defined as ρ'_{xy}/ρ^2) changes as impurities are added to increase $1/\tau$ (and ρ) (*3*, *7*). A dissipationless AHE current implies that $\rho'_{xy} \sim \rho^\alpha$, with $\alpha = 2$. By contrast, in the skew scattering model, $\alpha = 1$.

Tests based on measurements at high temperatures T (77 to 300 K) yield exponents in the range $\alpha_{exp} = 1.4$ to 2.0 (*18*, *19*). However, it has been argued (*20*) that at high T, both models in fact predict $\alpha = 2$, a view supported by detailed calculations (*21*). To be meaningful, the test must be performed in the impurity-scattering regime over a wide range of ρ. Unfortunately, in most ferromagnets, ρ'_{xy} becomes too small to measure accurately at low T. Results on α in the impurity-scattering regime are very limited.

The copper-chromium selenide spinel $CuCr_2Se_4$, a metallic ferromagnet with a Curie temperature $T_C \sim 430$ K, is particularly well suited for testing the AHE. Substituting Se with Br in $CuCr_2Se_{4-x}Br_x$ decreases the hole density n_h (*22*). However, because the coupling between local moments on Cr is primarily from 90° superexchange along the Cr-Se-Cr bonds (*23*), this does not destroy the magnetization. We have grown crystals of $CuCr_2Se_{4-x}Br_x$ by chemical vapor transport (*24*). When x is increased from 0 to 1 in our crystals, n_h decreases by a factor of ~30 while T_C decreases from 430 K to 230 K (Fig. 1A). The saturated magnetization M_s at 5 K corresponds to a Cr moment that actually increases from 2.6 to 3 μ_B (Bohr magneton) (Fig. 1B).

As shown in Fig. 1C, all samples except the ones with $x = 1.0$ lie outside the localization regime. In the "metallic" regime, the low-T resistivity increases by a factor of ~270 as x increases from 0 to 0.85; this increase is predominantly due to a decrease in τ by a factor of 70. The hole density n_h decreases by only a factor of 4. In the localization regime ($x = 1.0$), strong disorder causes ρ to rise gradually with decreasing T. We emphasize, however, that these samples are not semiconductors (ρ is not thermally activated, and $n_h = 1.9 \times 10^{20}$ cm^{-3} is degenerate).

The field dependence of the total Hall resistivity (Eq. 2) is shown in Fig. 2 for $x = 0.25$ and $x = 1.0$ [see (*24*) for measurement details]. The steep increase in $|\rho_{xy}|$ in weak H reflects the rotation of domains into alignment with **H**. Above the saturation field H_s, when ρ'_{xy} is constant, the small ordinary Hall term R_0B is visible as a linear background (*24*). As in standard practice, we used R_0 measured above T_C to find the n_h plotted in Fig. 1A.

By convention, the T dependence of the AHE signal is represented by the anomalous Hall coefficient $R_s(T)$ defined by $\rho'_{xy} = R_s\mu_0M$ (where μ_0 is the vacuum permeability). By scaling the

[1]Department of Physics, [2]Department of Chemistry, [3]Princeton Materials Institute, Princeton University, Princeton, NJ 08544, USA.

*Present address: Center for Crystal Science and Technology, University of Yamanashi, 7 Miyamae, Kofu, Yamanashi 400-8511, Japan.

†To whom correspondence should be addressed. E-mail: npo@princeton.edu

ρ'_{xy}-H curve against the M-H curve measured at each T, we have determined (*24*) R_s versus T in each of the samples studied (Fig. 3). The introduction of Br causes the R_s versus T profiles to change markedly. In the undoped sample (x = 0), R_s is positive and monotonically decreasing below 360 K, as is typical in high-purity ferromagnets (Fig. 3B). Weak doping (x = 0.1) produces a negative shift in R_s and a finite negative value at low T. Increasing the doping to x = 0.25 leads to an R_s profile that is large, negative, and nearly independent of T below 50 K (Fig. 3B). At mid-range doping and higher ($x \geq 0.5$), the magnitude of R_s increases steeply, but now in the positive direction. At maximum doping (x = 1), the value of R_s at 5 K is very large, corresponding to $\rho'_{xy} \sim 700$ μΩ·cm (Fig. 2B).

Our focus is on the low-T values of ρ'_{xy} where impurity scattering dominates. At 5 K, ρ'_{xy} is too small to be resolved in the sample with x = 0. As x increases to 1, the absolute magnitude $|\rho'_{xy}|$ at 5 K increases by more than three orders of magnitude (hereafter, ρ'_{xy} refers to the saturated value measured at 2 T or higher). It is noteworthy that ρ'_{xy} is negative at low doping ($0 < x < 0.4$) but becomes positive for $x > 0.5$. Initially, the sign change seemed to suggest to us that there might exist two distinct mechanisms for the AHE in this system. As more samples were studied, however, it became apparent that irrespective of the sign, the magnitude $|\rho'_{xy}|$ versus ρ falls on the same curve over several decades (Fig. 4), providing strong evidence that the same AHE mechanism occurs in both sign regimes. We focus first on the magnitude $|\rho'_{xy}|$ versus ρ, and discuss the change in sign later.

It is worth emphasizing that σ'_{xy} is proportional to the carrier density n_h (see Eq. 1). For our goal of determining whether the AHE current is dissipationless, it is clearly necessary to factor out n_h before comparing ρ'_{xy} against ρ. Hence, we divide $|\rho'_{xy}|$ by n_h. We refer to σ'_{xy}/n_h as the normalized AHE conductivity (*24*).

Figure 4 shows $|\rho'_{xy}|/n_h$ versus ρ in log-log scale for all samples investigated [except x = 0 (*24*)]. Over several decades, the data fit well to $|\rho'_{xy}|/n_h = A\rho^{\alpha}$ with $\alpha = 1.95 \pm 0.08$ (because M_s is nearly insensitive to x, Fig. 4 also gives $R_s/n_h \sim \rho^2$). This immediately implies that the normalized AHE conductivity σ'_{xy}/n_h at 5 K is dissipationless. Increasing ρ by a factor of ~100 leaves the AHE current per carrier unchanged to our measurement accuracy [see (*24*) for a discussion of our resolution]. As noted, the two samples with x = 1 are in the localization regime. The fact that their points also fall on the line implies that the dissipationless nature of the normalized AHE current extends beyond the Bloch-state regime (where most AHE theories apply) into the weak localization regime, where much less has been done. This supports recent theories (*10*, *11*, *17*) that the anomalous-velocity origin is topological in nature and is equally valid in the Bloch and localization regimes.

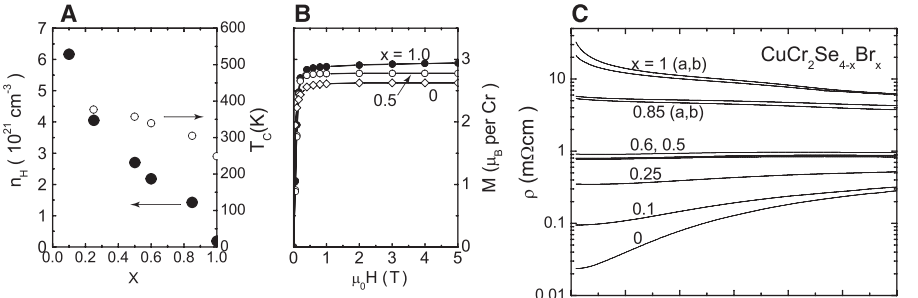

Fig. 1. (**A**) Hole density n_h (solid circles) in $CuCr_2Se_{4-x}Br_x$ versus x determined from R_0 at 400 K (one hole per formula unit corresponds to $n_h = 7.2 \times 10^{21}$ cm^{-3}). The Curie temperature T_C is shown as open circles. (**B**) Curves of the magnetization M versus H at 5 K in three samples (x values indicated). The saturation value $M_s = 3.52 \times 10^5$ A/m for x = 0, 3.72×10^5 A/m for x = 0.5, and 3.95×10^5 A/m for x = 1.0. (**C**) Resistivity ρ versus T in 10 samples with Br content x indicated (*a* and *b* indicate different samples with the same x). Values of n_h in all samples fall in the metallic regime (for x = 1, $n_h = 1.9 \times 10^{20}$ cm^{-3}).

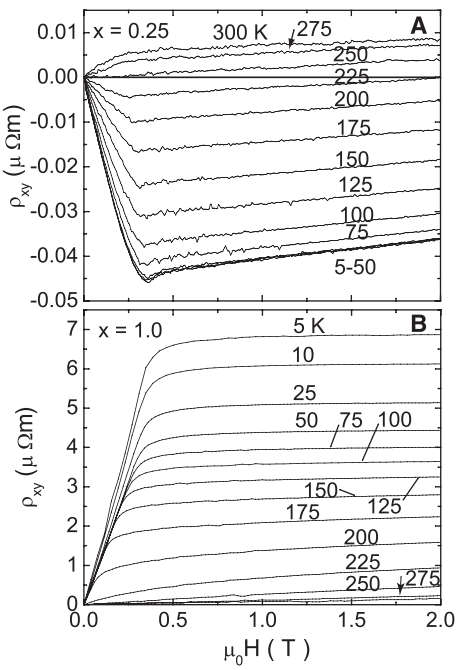

Fig. 2. Curves of the observed Hall resistivity $\rho_{xy} = R_0B + R_s\mu_0M$ versus H (at temperatures indicated) in $CuCr_2Se_{4-x}Br_x$ with x = 0.25 (**A**) and x = 1.0 (**B**). In (A), the anomalous Hall coefficient R_s changes sign below 250 K, becomes negative, and saturates to a constant value below 50 K. However, in (B), R_s is always positive. At low T, it rises to very large values (note difference in scale).

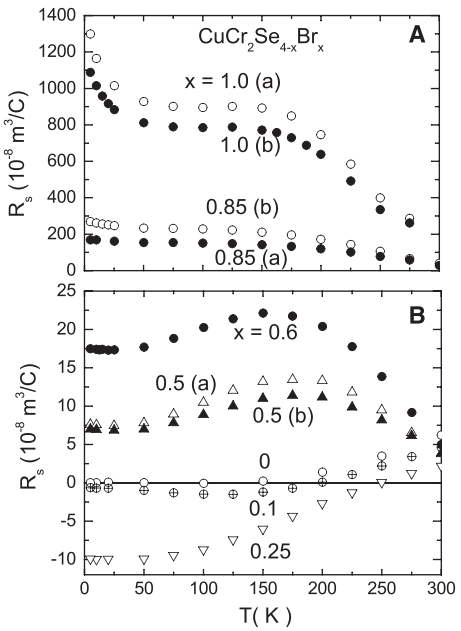

Fig. 3. (**A**) Values of R_s extracted from the curves of ρ_{xy} and M versus H measured at each T in $CuCr_2Se_{4-x}Br_x$, with values of x indicated (*a* and *b* refer to different crystals with the same x). (**B**) The corresponding curves for x = 0, 0.1, 0.25, and 0.5 (two crystals *a* and *b*). The values of R_s at 5 K are negative at small x (< 0.4), but as x increases, R_s rapidly rises to large positive values.

The sign change at $x \sim 0.4$ is reminiscent of sign changes observed in ferromagnetic alloys (versus composition). The common feature is that doping drives the Fermi energy ε_F across the overlap between two narrow bands derived from distinct transition-metal elements. In the alloy $Ni_{1-x}Fe_x$, the band derived from Fe 3*d* states lies just above the 3*d* band of Ni. As ε_F crosses the overlap, ρ'_{xy} changes from negative to positive. Similar sign changes are observed in Au-Fe and Au-Ni alloys. It has been pointed out (*2*) that the effective spin-orbit parameter λ in Eq. 1 changes sign whenever ε_F moves between overlapping narrow bands. A similar effect is implied in Noziéres and Lewiner's calculation (*9*). Band-structure calculations (*25*) on $CuCr_2Se_4$ reveal that ε_F lies in a hole-like band of mostly Cu 3*d* character strongly admixed with Cr 3*d* states lying just above. We infer that as ε_F rises with increasing Br content, the conduction states acquire more Cr 3*d* character at the expense of Cu 3*d*, triggering

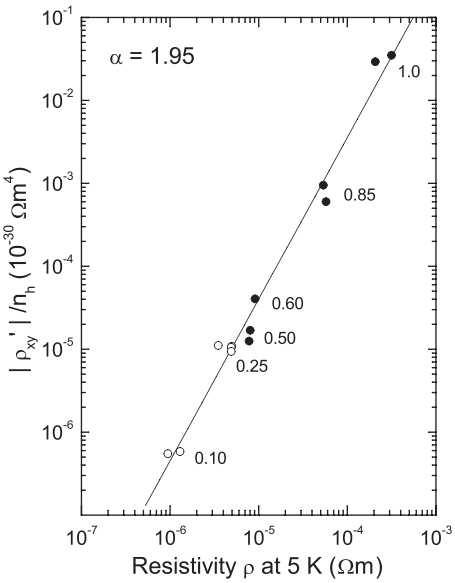

Fig. 4. The normalized quantity $|\rho'_{xy}|/n_h$ versus ρ (at 5 K) in a log-log plot (ρ'_{xy} is measured at 2 T and 5 K). The 12 samples (with doping x indicated) include ones with negative ρ'_{xy} (open circles) and positive ρ'_{xy} (solid circles). The undoped sample ($x = 0$) is not shown because ρ'_{xy} at 5 K is unresolved in our experiment (*24*). The least-squares fit gives $|\rho'_{xy}|/n_h = A\rho^{\alpha}$ with $\alpha = 1.95 \pm 0.08$ and $A = 2.24 \times 10^{-25}$ (SI units).

a sign change in λ. The sign change (negative to positive with increasing x) is consistent with that observed in $Ni_{1-x}Fe_x$. A change in sign of the AHE conductivity at band crossings is also described in recent theories (*10*).

We now discuss the relevance of our findings to spin current production. To produce fully polarized spin currents, it is ideal to use "half metals" (ferromagnets in which all conduction electrons are, say, spin-up). However, only a few examples are known (*26*). Alternate schemes based on elemental ferromagnets have been proposed (*16*). As is evident from Eq. 1, anomalous-velocity theories predict that $\mathbf{J}_H$ depends on the carrier spin $\mathbf{S}$. If a beam of electrons with spin populations $n_\uparrow$ and $n_\downarrow$ enters a region of fixed $\mathbf{M}$, the spin-up and spin-down electrons are deflected in opposite directions transverse to $\mathbf{E}$, just as in the classic Stern-Gerlach experiment. This results in a Hall charge current proportional to the difference between the spin populations, namely $\mathbf{J}_H \sim (n_\uparrow - n_\downarrow)$. More important, this also produces a fully polarized spin-Hall current $\mathbf{J}_s$ proportional to the sum $(n_\uparrow + n_\downarrow)$. Hence, in a ferromagnet that is not a half metal, the spin-Hall current is fully polarized according to these theories. By contrast, in skew-scattering theories, $\mathbf{J}_H$ depends on the direction of the local moment $\mathbf{m}_i$ on the impurity but not the spin of the incident electron; that is, both $\mathbf{J}_H$ and $\mathbf{J}_s \sim (n_\uparrow - n_\downarrow)$.

In confirming that the normalized AHE current is dissipationless over a multidecade change in ρ, we verify a specific prediction of the anomalous-velocity theories and resolve a key controversy in ferromagnets. The implication is that fully polarized spin-Hall currents are readily generated in ferromagnets (at low T) by simply applying $\mathbf{E}$. Although this realization does not solve the conductivity-mismatch problem at interfaces (*27*), it may greatly expand the scope of experiments on the properties of spin currents.

References and Notes

1. C. Hurd, *The Hall Effect in Metals and Alloys* (Plenum, New York, 1972), pp. 153–182.
2. L. Berger, G. Bergmann, in *The Hall Effect and Its Applications*, C. L. Chien, C. R. Westgate, Eds. (Plenum, New York, 1980), pp. 55–76.
3. R. Karplus, J. M. Luttinger, *Phys. Rev.* **95**, 1154 (1954).
4. J. M. Luttinger, *Phys. Rev.* **112**, 739 (1958).
5. E. N. Adams, E. I. Blount, *J. Phys. Chem. Solids* **10**, 286 (1959).
6. J. Smit, *Physica* (*Amsterdam*) **21**, 877 (1955).
7. L. Berger, *Phys. Rev. B* **2**, 4559 (1970).
8. S. K. Lyo, T. Holstein, *Phys. Rev. B* **9**, 2412 (1974).
9. P. Noziéres, C. Lewiner, *J. Phys.* (*France*) **34**, 901 (1973).
10. M. Onoda, N. Nagaosa, *J. Phys. Soc. Jpn.* **71**, 19 (2002).
11. T. Jungwirth, Q. Niu, A. H. MacDonald, *Phys. Rev. Lett.* **88**, 207208 (2002).
12. H. Ohno, *Science* **281**, 951 (1998).
13. P. Matl *et al.*, *Phys. Rev. B* **57**, 10248 (1998).
14. J. Ye *et al.*, *Phys. Rev. Lett.* **83**, 3737 (1999).
15. Y. Taguchi, Y. Oohara, H. Yoshizawa, N. Nagaosa, Y. Tokura, *Science* **291**, 2573 (2001).
16. J. E. Hirsch, *Phys. Rev. Lett.* **83**, 1834 (1999).
17. S. Murakami, N. Nagaosa, S.-C. Zhang, *Science* **301**, 1348 (2003).
18. C. Kooi, *Phys. Rev.* **95**, 843 (1954).
19. W. Jellinghaus, M. P. DeAndres, *Ann. Phys.* **7**, 189 (1961).
20. J. Smit, *Phys. Rev. B* **8**, 2349 (1973).
21. S. K. Lyo, *Phys. Rev. B* **8**, 1185 (1973).
22. K. Miyatani *et al.*, *J. Phys. Chem. Solids* **32**, 1429 (1971).
23. J. B. Goodenough, *J. Phys. Chem. Solids* **30**, 261 (1969).
24. See supporting data on *Science* Online.
25. F. Ogata, T. Hamajima, T. Kambara, K. I. Goondaira, *J. Phys. C* **15**, 3483 (1982).
26. R. J. Soulen Jr. *et al.*, *Science* **282**, 85 (1998).
27. G. Schmidt, D. Ferrand, L. W. Molenkamp, A. T. Fiolip, B. J. van Wees, *Phys. Rev. B* **62**, R4790 (2000).

28. Supported by NSF Materials Research Science and Engineering Center grant DMR 0213706.

Supporting Online Material

www.sciencemag.org/cgi/content/full/303/5664/1647/DC1
Materials and Methods
Figs. S1 and S2
References

5 December 2003; accepted 4 February 2004

Glass Formation at the Limit of Insufficient Network Formers

S. Kohara,[1] K. Suzuya,[2] K. Takeuchi,[3] C.-K. Loong,[4]* M. Grimsditch,[4] J. K. R. Weber,[5] J. A. Tangeman,[5] T. S. Key[5]

Inorganic glasses normally exhibit a network of interconnected, covalent-bonded, structural elements that has no long-range order. In silicate glasses, the network formers are based on SiO_4 tetrahedra interconnected through oxygen atoms at the corners. Conventional wisdom implies that alkaline and alkaline-earth orthosilicate materials cannot be vitrified, because they do not contain sufficient network-forming SiO_2 to establish the needed interconnectivity. We studied a bulk magnesium orthosilicate glass obtained by containerless melting and cooling. We found that the role of network former was largely taken on by corner and edge sharing of highly distorted, ionic Mg-O species that adopt 4-, 5-, and 6-coordination with oxygen. The results suggest that similar glassy phases may be found in the containerless environment of interstellar space.

Conventional silicate glasses contain sufficient SiO_2 so that the average number of corner-sharing oxygen atoms per SiO_4 tetrahedron is greater than two, resulting in a three-dimensional (3D) glass-forming network. Other constituent oxide components behave effectively as network modifiers. In so-called invert glasses, where the relative amount of SiO_2 is reduced to an extent that, on average, only isolated SiO_4 and Si_2O_7 dimers exist, the short-range order structure and the relaxation phenomena undergo drastic changes (*1*). Previously studied invert glasses had rather complex compositions, which prohibited a detailed understanding of the short-range structure (*1*). It is therefore important to investigate vitreous forsterite (v-Mg_2SiO_4), which is a simple but unusual invert glass and a model system for nonequilibrium, low-silica-content binary melts.

Experimental studies of v-Mg_2SiO_4 are difficult because of its high melting point (~2150 K) and our inability to form a bulk glass using conventional melt and quench

[1]Japan Synchrotron Radiation Research Institute, Mikazuki, Sayo, Hyogo 679–5198, Japan. [2]Japan Atomic Energy Research Institute, Tokai, Naka, Ibaraki 319–1195, Japan. [3]Tokyo University of Science, Oshamanbe, Yamakoshi, Hokkaido 049–3514, Japan. [4]Argonne National Laboratory, Argonne, IL 60439–4814, USA. [5]Containerless Research Inc., 906 University Place, Evanston, IL 60201–3149, USA.

*To whom correspondence should be addressed. E-mail: ckloong@anl.gov